On the Infusion of a Therapeutic Agent Into a Solid Tumor Modeled as a Poroelastic Medium

Alessandro Bottaro[1]
e-mail: alessandro.bottaro@unige.it

Tobias Ansaldi

Research Center for Materials Science and Technology,
Università di Genova,
1, via Montallegro,
16145 Genova, Italy

The direct infusion of an agent into a solid tumor, modeled as a spherical poroelastic material with anisotropic dependence of the tumor hydraulic conductivity upon the tissue deformation, is treated both by solving the coupled fluid/elastic equations, and by expressing the solution as an asymptotic expansion in terms of a small parameter, ratio between the driving pressure force in the fluid system, and the elastic properties of the solid. Results at order one match almost perfectly the solutions of the full system over a large range of infusion pressures. Comparison with experimental results is acceptable after the hydraulic conductivity of the medium is properly calibrated. Given the uncertain estimates of some model constants, the order zero solution of the expansion, for which fluid and porous matrix are decoupled, yields acceptable values and trends for all the physical fields of interest, rendering the coupled analysis (in the limit of small displacements) of little use. When the deformation of the tissue becomes large nonlinear elasticity theory must be resorted to. [DOI: 10.1115/1.4007174]

Keywords: solid tumor, infusion, poroelasticity, asymptotic model, fluid mechanics

1 Introduction

In recent years it has become common to shrink solid tumors before surgery via intratumoral injection of chemotherapeutic drugs, to allow cleaner/simpler/less destructive removal, or to render operable possibly inoperable tumors. Efficient delivery of a therapeutic agent within a solid tumor via intratumoral infusion requires a thorough understanding of the fluid dynamics in the gel-like region between cells (the *interstitium*). A number of physiological barriers opposes the infusion: the abnormally elevated density of cancer cells limits drug transport by constricting intratumoral blood vessels; the high interstitial fluid pressure (IFP) which occurs within the tumor and the lack of functional lymphatics hamper convective transport of the agents to the interstitium; and the tumor microvasculature is leaky. The main obstacle to efficient delivery is believed to be the high IFP (values up to 50 mmHg have been reported in solid tumors [1–4]); it can produce some reabsorption of fluid by the capillary network with the consequence that not all the therapeutic agent injected diffuses within the tumor tissues.

It is common to model the problem of the transport of drugs and nutrients within a solid tumor by considering it as a fluid-saturated porous medium, characterized by the hydraulic conductivity K of the tissue (ratio between the permeability of the medium and the dynamic viscosity of the fluid) and by its Lamé coefficients, G and λ. Assuming negligible lymphatic drainage, the parameters needed to describe transvascular fluid exchange, within the Starling's law assumption, are the hydraulic conductivity of the capillary walls, L_p, the vascular surface area per unit volume, S/V, and the effective vascular pressure, p_e. Macroscopic parameters can, in principle, be inferred from homogenizing the microscopic features of the tumor, i.e., its morphology as a micro-structured material, with fiber matrix, proteins, fluid in the interstitial matrix, and including the fluid exchange with the capillaries embedded in the interstitium (see [5] for recent progress on this). A more common approach is to infer values of the governing parameters from in vivo and in vitro measurements. Smith and Humphrey [6] provide a review of measured values from the literature.

The rate of fluid flow within the tumor depends on the value of K of the tissues which can, in principle, be strongly altered by the deformation of the tissues themselves. It has been found [7] that variations of the hydraulic conductivity by several orders of magnitude may take place with a fourfold increase of the infusion pressure, as a result of tissue expansion and compression. Hence, the coupling between the deformation of the tumor and its conductivity appears to be important, and the use of poroelasticity theory has been proposed, see for example, [8,9]. Whereas various empirical relations for $K = K(u)$, with u the displacement of the solid, are present in the literature [10,11], only McGuire et al. [12] consider a nonlinear, anisotropic relation.

In this work we follow the lead of McGuire et al. [12] to study the intratumoral infusion of a therapeutic agent into an isolated solid tumor of spherical shape, i.e., a tumor that is not surrounded by normal tissue. A perturbation approach is proposed within the linear elastic approximation, with the solution expressed in term of powers of a small dimensionless parameter δ, defined as the ratio between an effective pressure at the infusion site and the tissue solid properties (expressed via a linear combination of G and λ). A comparison between results obtained with the full model and with the perturbation analysis (up to order δ) provides an indication on the range of applicability of the asymptotic approach.

2 The Model

Tumors are strongly heterogeneous and are often modeled as being formed by concentric layers of tissue (eventually including a necrotic core) of thickness defined by the proliferation/quiescent activity of the cancer cells. Here, we consider a spherical tumor of radius R, a compressible medium modeled as an elastic network of communicating, fluid-filled pores, whose sources of radial inhomogeneity are in the hydraulic conductivity of the tumor interstitium, K, and in the hydraulic conductivity of the capillary walls, L_p. Our modeling assumptions are as follows: a drug is infused at the center by a needle, and the tissue is cored out, creating a small fluid cavity of radius a around the needle tip (cf. Fig. 1). As fluid is injected, the tissue swells mildly and, at the steady state, the fluid fills a spherical cavity of radius a'. Likewise, the radius of the tumor becomes R' in steady infusion conditions. This model replicates the one proposed by Basser [13] and used by many authors afterwards, with spherical symmetry maintained. The stress tensor $\mathbf{T}$ is related to the strain tensor $\boldsymbol{\varepsilon}$ by a linear constitutive law,

$$\mathbf{T} = -p\mathbf{I} + \lambda(\nabla \cdot \mathbf{u})\mathbf{I} + 2G\boldsymbol{\varepsilon} \tag{1}$$

with p the IFP, and $\boldsymbol{\varepsilon} = (\nabla\mathbf{u} + \nabla\mathbf{u}^T)/2$ (the superscript T denotes transpose operation). We assume that the displacement vector, $\mathbf{u}$, has only a nonzero radial component, u, so that the only nonvanishing components of $\boldsymbol{\varepsilon}$ are $\varepsilon_{rr} = du/dr$ and $\varepsilon_{\theta\theta} = \varepsilon_{\phi\phi} = u/r$, r being the radial coordinate (in the following when r is used as a subscript a derivation is intended, except when the subscript denotes the component of a tensor, for example, σ_{rr} or ε_{rr}). By setting to zero the divergence of $\mathbf{T}$, we obtain the equilibrium equation, whose radial component is

$$(2G + \lambda)(u_r + 2u/r)_r = p_r \tag{2}$$

[1]Corresponding author.

Contributed by the Bioengineering Division of ASME for publication in the JOURNAL OF BIOMECHANICAL ENGINEERING. Manuscript received December 9, 2011; final manuscript received July 6, 2012; accepted manuscript posted July 18, 2012; published online August 6, 2012. Assoc. Editor: Dalin Tang.

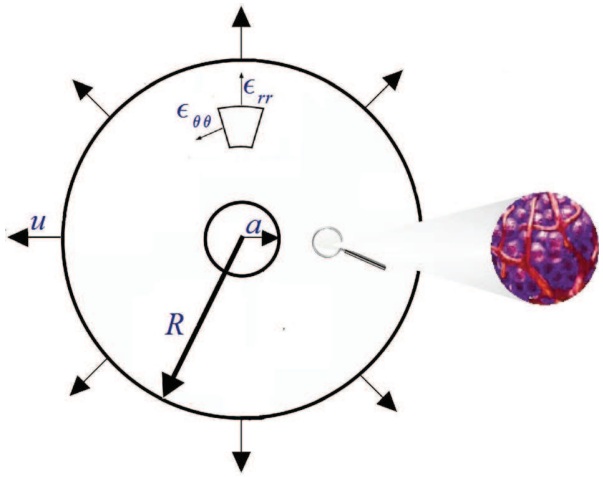

Fig. 1 Sketch of the section of a solid tumor of spherical shape. The magnified view on the right shows a detail of the porous interstitium, with the micro-vasculature created around the tumor cells.

The conservation of mass in the fluid phase within the Darcy flow assumption (see, e.g. [6]) is

$$-\left(r^2 K p_r\right)_r / r^2 = L_p(p_e - p)S/V \tag{3}$$

with the right-hand side, the Starling's law term, which can act as either a source or a sink because of the leakiness of the tumor microvasculature. The tumor vasculature is structurally and functionally abnormal, undergoing continual adaptation in response to blood flow and metabolite levels. The common practice of assuming a constant value of the effective vascular pressure, p_e, can be questioned in the presence of significant transvascular fluid exchange; however, given the extreme difficulty in modeling the tumor microvascular circulation (see [14] for recent progress) and in order to keep the present problem tractable, we have decided to maintain p_e constant and to account for the heterogeneous distribution of vessels only through a variable hydraulic conductivity of the capillary walls, L_p. To model the increased activity of cancer cells towards the outer boundary of the tumor, where they co-opt host vessels to obtain nutrients for their growth and sprout new vessels from existing ones, we assume that L_p varies with r as

$$L_p = L_{p0} f(r/R) \tag{4}$$

with L_{p0} a reference value and $f(r/R)$ a dimensionless function ranging from zero to one, which can only increase (or eventually remain constant) with r. This should not be taken to mean that newly formed blood vessels have larger conductivity than existing ones, it is rather a way to model (in a continuous manner) the fluid-exchange-activity of the microvasculature, from the inner (possibly necrotic and hypoxic) core, through the viable tumor tissue, and to the outer proliferating region. A similar (albeit discrete) approach is used, for example by Smith and Humphrey [6].

To model the anisotropic dependence of the hydraulic conductivity K on the tissue deformation, when the volume fraction of fibers and cells in the tissue is large, we assume, following McGuire et al. [12], that

$$K = K_0 \exp\{M[\alpha\varepsilon_{rr} + (1-\alpha)\varepsilon_{\theta\theta}]\} \tag{5}$$

with K_0, M, and α, model constants. The equations are closed by boundary conditions, i.e.,

$$p(R') = 0; \quad p(a') = p_{\text{infusion}}; \quad (2G+\lambda)u_r(R') + 2\lambda u(R')/R' = 0;$$
$$-p(a') + (2G+\lambda)u_r(a') + 2\lambda u(a')/a' = -p_{\text{infusion}} \tag{6}$$

The latter two relations specify, respectively, the absence of radial contact stresses at the tumor margins $r = R'$, and the continuity of the radial components of the stress across the interface in $r = a'$ between the cavity and the porous matrix [15]. Since a' and R' are a priori unknown, they must be solved for as part of the procedure, in an iterative manner. We thus solve the equations repeatedly, enforcing the boundary conditions (6) at $R' = R + u(R)$, and $a' = a + u(a)$, with $u(a)$ and $u(R)$ coming from the preceding iteration, and declare convergence whenever the variations of R' and a' between two successive iterations are below a given threshold (taken to be machine accuracy).

Normalization of equations and boundary conditions brings out the relevant parameters of this model. We thus scale the IFP with $(p_{\text{infusion}} - p_e)$, the displacement u and the radial coordinate r with R, and the hydraulic conductivity K with K_0, isolating two dimensionless parameters,

$$\delta = (p_{\text{infusion}} - p_e)/(2G+\lambda) \tag{7}$$

$$\gamma^2 = \left(L_{p0}/K_0\right)R^2 S/V \tag{8}$$

The first parameter characterizes the ratio between the driving pressure forces in the fluid system and the elastic properties of the solid; the second parameter measures the relative importance of the resistance to interstitial percolation with respect to the resistance to transcapillary fluid exchange [1,16]. Typically δ is much smaller than one, whereas γ is of order one.

The equations in terms of dimensionless variables read

$$\left(u_r + 2u/r\right)_r = \delta p_r \tag{9}$$

$$\left(r^2 K p_r\right)_r = r^2\gamma^2(p - p_e)f(r) \tag{10}$$

$$K = \exp\{M[\alpha u_r + (1-\alpha)u/r]\} \tag{11}$$

with boundary conditions,

$$p(R'/R) = 0; \quad p(a'/R) = p_{\text{infusion}};$$
$$u_r(R'/R) + 2\lambda/(2G+\lambda)u(R'/R)/R' = 0;$$
$$u_r(a'/R) + 2\lambda/(2G+\lambda)u(a'/R)/a' = 0 \tag{12}$$

Equations (9)–(12) are solved by a finite difference second order iterative scheme, yielding solutions for p, the hydraulic conductivity K, the Darcy flux $q = -K p_r$ and the flow rate Q of the therapeutic agent through the tumor, for parameters corresponding to some of the measurements by McGuire et al. [12]. We denote by Q_{infusion} the value of Q at $r = a'$, i.e., $Q_{\text{infusion}} = 4\pi a'^2 q|_{r=a'} = -4\pi a'^2 K p_r|_{r=a'}$.

3 The Perturbation Approach

A second approach to the solution of the problem begins, following Bonfiglio et al. [17], by expanding the dependent variables into powers of δ as

$$u = u_0 + \delta u_1 + O\left(\delta^2\right)$$

$$p = p_0 + \delta p_1 + O\left(\delta^2\right)$$

$$K = K_0 + \delta K_1 + O\left(\delta^2\right)$$

When there is no pressure imbalance ($\delta \equiv 0$) Eq. (9) reduces to $(u_r + 2\,u/r)_r = 0$ which yields the (trivial) result $u \equiv 0$ (and correspondingly $K \equiv 1$). This is physically obvious since the displacement u is induced by the pressure imbalance δ, so that u must be of order δ, i.e., $u_0 = 0$, $K_0 = 1$. The unperturbed solution for the pressure, p_0, is simply found by solving

$$\left(r^2 p_{0r}\right)_r = r^2\gamma^2(p_0 - p_e)f(r) \tag{13}$$

together with $p_0(1) = 0$ and $p_0(a) = p_{\text{infusion}}$. In the $L_p = L_{p0}$ limit we have

$$p_0 = p_e + Ae^{\gamma r}/r + Be^{-\gamma r}/r \tag{14}$$

with A and B easily available from the boundary conditions. For $f(r)$ not constant and equal to one, the zeroth order pressure field can be found by numerical integration of Eq. (13); this yields an order 0 solution which is uniformly valid in r, i.e., the problem being considered is a *regular perturbation* problem. From p_0 it is easy to recover the leading order Darcy flux q_0 and flow rate Q_0. At order 1, the equations are

$$(u_{1r} + 2u_1/r)_r = p_{0r} \tag{15}$$

$$\left(r^2 p_{1r} + r^2 K_1 p_{0r}\right)_r = r^2 \gamma^2 p_1 f(r) \tag{16}$$

with $K_1 = M[\alpha\, u_{1r} + (1-\alpha)\, u_1/r]$, and boundary conditions

$$\begin{aligned} p_1(1) &= -u_1(1) p_{0r}(1) \\ p_1(a) &= -u_1(a) p_{0r}(a) \\ u_{1r}(1) &+ 2\lambda/(2G+\lambda) u_1(1) = 0 \\ u_{1r}(a) &+ 2\lambda/(2G+\lambda) u_1(a)/a = 0 \end{aligned} \tag{17}$$

(a is now normalized by the outer unperturbed radius, and is thus dimensionless), obtained by Taylor expanding the boundary conditions in Eq. (6) around the unperturbed positions, and collecting terms of order δ. The variables p_1, K_1, and u_1, as well as q_1 and the infusion flow rate at order δ, can be obtained by a central difference numerical method, similar to that used for Eqs. (9)–(12). In both cases we have employed a large number of uniformly distributed radial grid points (up to 6000) to ensure that all results presented are grid-converged.

4 Results

The configurations which can be examined with the present asymptotic model are all those for which δ is "small". This is not an uncommon situation, and is encountered often (i.e., Smith and Humphrey [6] for which $\delta = 0.15$, Sarntinoranont et al. [9] for which $\delta = 0.16$ when $p_e = 11.25$ mmHg, and Netti et al. [8] for which $\delta = 0.012$, etc.). Furthermore, we will show in the following that "small" does not necessarily mean infinitesimal, rendering the present approach widely applicable.

To set ideas we consider the situation examined in the study of 4T1 cell lines by McGuire et al. [12]. These lines had the highest collagen concentration among the tested ones, and showed a strongly nonlinear relation between the infusion pressure and the infusion rate. They were murine mammary carcinoma cell lines, injected subcutaneously into mice. After the tumor had grown to a diameter of the order of the centimeter, a solution was infused into the center of the tumor with a needle, until a small fluid cavity approximately equal to the needle radius was formed. From that point on, increasing and measuring the infusion pressure, McGuire et al. [12] could measure the corresponding flow rate of the solution entering the tissue. Errors in the measured pressures could be quantified to be less than 3.7 mmHg.

In Tables 1 and 2, a list of all of the parameters in McGuire et al.'s [12] experiments is provided together with those employed in the present simulations (unless otherwise indicated). We still need to define the function $f(r)$ in the model, and we consider three different choices, denoted as cases 1, 2, and 3; the most important difference among the cases is the degree to which the function is concentrated at $r = 1$, representing the increase in leakiness of the capillary network there. Case 1 assumes a constant value of $L_p = L_{p0}$, i.e., $f(r) = 1$; in case 2 it is assumed that $f(r)$ increases radially outwards as $f(r) = \exp[b(r-1)/(1-a)]$, with $b = \log(10)$; the value of L_p at $r = R$ is equal to L_{p0} and it is ten times larger than the corresponding value at $r = a$. The factor of 10 is arbitrary, but within the range of values reported in the literature [1,6]. In the third case we make the hypothesis that transvascular fluid exchange is concentrated near the tumor outer margins, possibly as a result of strong localized angiogenesis, so that $f(r) = \exp[-150(r-1)^2]$. These three distributions cover a large spectrum of configurations, and are plotted in Fig. 2. In Figs. 3 and 4 results are reported from simulations using the full model, i.e., Eqs. (9)–(12), at $\delta = 0.05$ (corresponding to $p_{\text{infusion}} = 27.5$ mmHg) and $\delta = 0.2$

Table 1 Dimensional variables and model parameters

Physical variable	Definition
$a = 0.18$ mm; $R = 5$ mm	Unperturbed radii of the cavity and of the spherical tumor
$p_e = 11.25$ mmHg	Effective vascular pressure [6]
$30\text{ mmHg} \le p_{\text{infusion}} \le 70\text{ mmHg}$	Range of values of the infusion pressure
$L_{p0} = 1.3332 \times 10^{-6}$ cm/(mmHg s)	Vascular conductivity at $r = R$ [6]
$S/V = 200\text{ cm}^2/\text{cm}^3$	Vascular surface area per unit volume [6]
$\lambda = 175$ mmHg, $G = 75$ mmHg	Lamé coefficients; they are related through the relation $\lambda = 2\,\nu\, G/(1-2\,\nu)$, with the Poisson ratio ν which is fixed at 0.35.
$K_0 = 3 \times 10^{-5}\text{ cm}^2/(\text{mmHg s})$	Model constant in Eq. (5). The literature typically reports smaller values for K_0, cf. [6]
$\alpha = 0.733$	Model constant in Eq. (5). The range of α is [0, 1]; the value $\alpha = 0.733$ provided the best fit with the experimental data in the model by McGuire et al. [12]
$M = 10$	Model constant in Eq. (5).

Table 2 Dimensionless parameters in the present simulations

a	δ (Eq. (7))	γ^2 (Eq. (8))	p_{infusion}
0.036	[0.05769, 0.1807]	2.2222	[1.1915, 1.6]

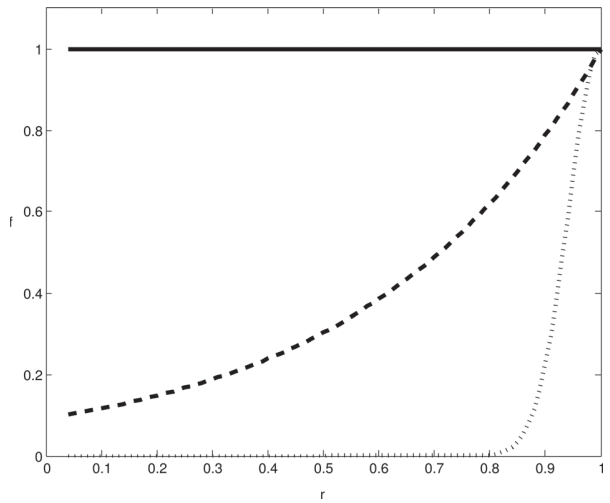

Fig. 2 Shape of the dimensionless function $f(r)$ (representing the hydraulic conductivity coefficient, L_p, of the capillary walls) for cases 1–3, as reported in the text. Case 1: solid line; case 2: dashed line; case 3: dotted line.

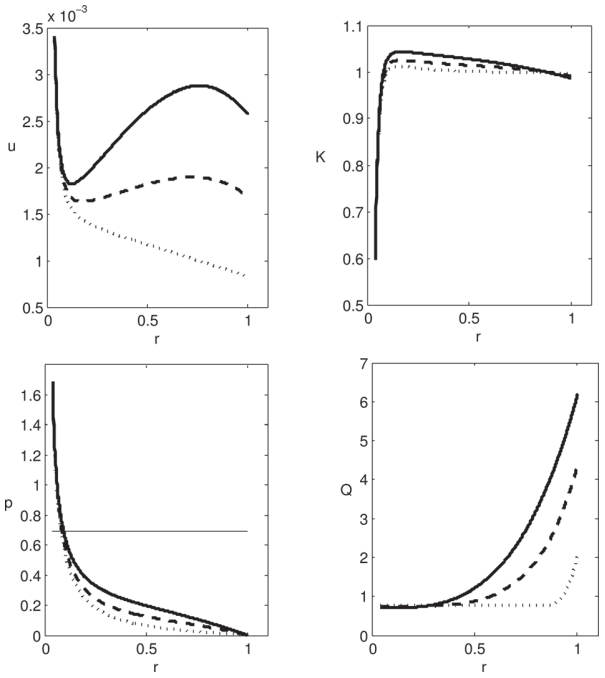

Fig. 3 Solution of the full model (in dimensionless form) for $\delta = 0.05$. From top left frame, and clockwise: radial distribution of the displacement *u*, of the hydraulic conductivity *K* of the tissue, of the flow rate *Q* through any given spherical surface at radius *r* (including transvascular fluid exchange), and of the IFP. Cases 1–3 with line styles as in Fig. 2 The thin horizontal line in the figure with the IFP denotes the dimensionless value of the effective vascular pressure.

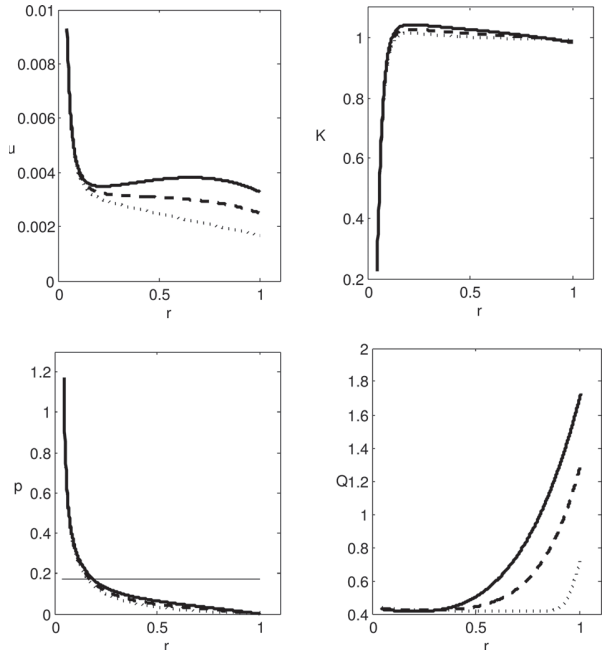

Fig. 4 Solution of the full model (in dimensionless form) for $\delta = 0.2$. From top left frame, and clockwise: radial distribution of the displacement *u*, of the hydraulic conductivity *K* of the tissue, of the flow rate *Q* through any given spherical surface at radius *r* (including transvascular fluid exchange), and of the IFP. Cases 1–3 with line styles as in Fig. 2 The thin horizontal line in the figure with the IFP denotes the dimensionless value of the effective vascular pressure.

($p_{\text{infusion}} = 76.25$ mmHg). As expected the deformation u is larger for larger infusion pressure. The trend of the u-curves with r varies with the case considered: it decreases rapidly near the infusion site for all cases, to eventually increase (case 1), settle (case 2) or slowly decrease (case 3); smaller radial displacements (and smaller flow rates Q) are associated with the reduced activity of the microvasculature towards the center of the tumor in cases 2 and 3. Perhaps unexpectedly the conductivity K of the tissue is but mildly affected by variations in the hydraulic conductivity of the capillary walls; in both Figs. 3 and 4 one observes a very steep increase of K from the infusion point, and a rapid equilibration around $K \approx 1$. The IFP is very large at the infusion site, but it decreases rapidly and monotonically from p_{infusion} to zero, the effect of L_p being minor; the IFP is thus smaller than the effective vascular pressure over a large range of r, which means that, under the conditions examined here, there is efficient transport of the drug to the tumor tissue. This is reflected also by the increase in the flow rate Q through the system for increasing radii, indicating extravasation of fluid from the vessels into the tumor interstitium, not balanced by reabsorption by the capillary system.

The rate of agent entering the tumor at $r = a'$ for varying values of the infusion pressure is displayed in Fig. 5, for the three cases of Fig. 2. It is interesting to observe that for the value of K_0 ($K_0 = 3 \times 10^{-5}$ cm^2/(mmHg s)) employed by McGuire et al. [12] our model overestimates the infusion rate. On the other hand, values of the average hydraulic conductivity typically much lower than 3×10^{-5} cm^2/(mmHg s) are often reported for neoplastic tissues (see, e.g., Swabb et al. [18] who measure in vitro values of 4×10^{-8} cm^2/(mmHg s), or Smith and Humphrey [6] who indicate a range between 4×10^{-9} cm^2/(mmHg s) and 2.5×10^{-6} cm^2/(mmHg s)). Therefore, in Fig. 5 we have also included results for the three cases of Fig. 2 when the value of K_0 is ten times smaller than that indicated by McGuire et al. [12], achieving a better match with experimental data. McGuire et al. [12] observed a

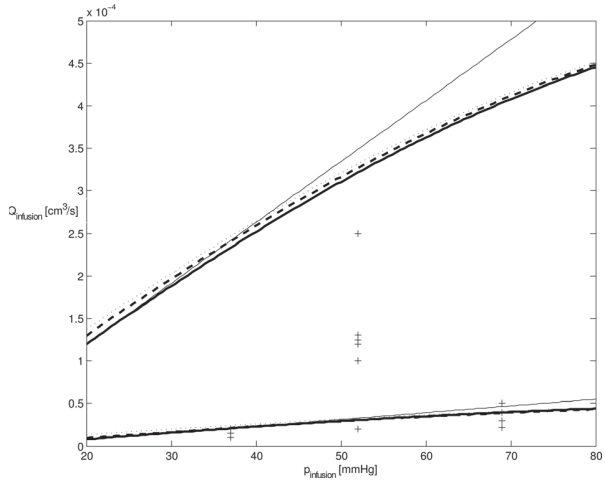

Fig. 5 Inflow rate at $r = a'$ as function of the infusion pressure (both variables are in dimensional form). Symbols are used to denote the experimental data points by McGuire et al. [12]. The three cases of Fig. 2 are plotted with the same line style used previously. The top curves refer to $K_0 = 3 \times 10^{-5}$ cm^2/(mmHg s); the bottom curves, closer to the experimental data, are for $K_0 = 3 \times 10^{-6}$ cm^2/(mmHg s). The order zero results of the asymptotic model in the $L_p = L_{p0}$ limit are also displayed, with thin solid lines; when L_p varies (as in Fig. 2) the leading order results are but mildly affected.

marked reduction of the infusion rate after the infusion pressure exceeds 50 mmHg (cf. their Fig. 4, bottom frame) and argued that the bell-shaped curve in the $p_{\text{infusion}} - Q_{\text{infusion}}$ plane is partly related to the formation of a thin membrane around the needle tip,

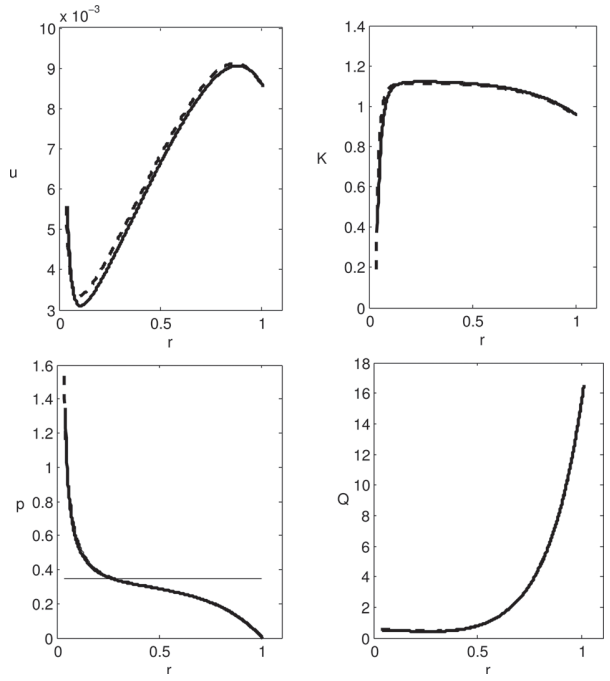

Fig. 6 Exact (thick solid lines), order zero (thin solid lines) and order one asymptotic results (dashed lines) in dimensionless form for $p_{infusion} = 43.75$ mmHg ($\delta = 0.1$) and $K_0 = 3 \times 10^{-6}$ cm^2/(mmHg s). The leading order value of u is zero and $K_0 = 1$ (not drawn). The horizontal line in the frame with the IFP denotes the effective vascular pressure.

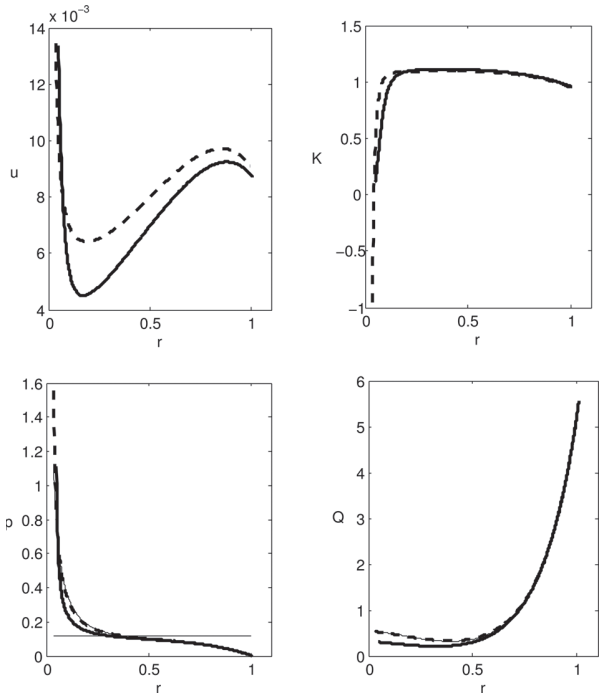

Fig. 7 Exact (thick solid lines), order zero (thin solid lines) and order one asymptotic results (dashed lines) in dimensionless form for $p_{infusion} = 108.75$ mmHg ($\delta = 0.3$) and $K_0 = 3 \times 10^{-6}$ cm^2/(mmHg s). The horizontal line in the frame with the IFP denotes the effective vascular pressure.

forcing the pressure in the cavity to be above a given threshold before intratumoral infusion can take place. The existence of a threshold pressure for infusion had been reported previously [19] and the mechanism still awaits a complete physical description. Another possible reason of discrepancy between the numerical results that we have obtained and those by McGuire et al. [12] is due to the neglect/account of fluid exchange between the interstitium and the blood vessels. Accounting for it, via the Starling's law term, we find that Q increases with r, with fluid filling the extra-cellular matrix and contributing to the increase of the strain. Figure 5 shows also results obtained from the asymptotic model at order zero, with constant $L_p = L_{p0}$ (i.e., results directly available from Eq. (14)). It is interesting to observe that, particularly at low infusion pressures, they do not differ much from the solutions of the full system (9)–(12), and are similarly affected by variations in K_0. As expected, the agreement between the exact solution of the full model and the leading order solution deteriorates with the increase of δ. Given the uncertainties in the estimate of the hydraulic conductivity, for practical purposes, in the limit of very small deformations, the leading order term of the expansion yields field values which are sufficiently accurate. On the other hand, for "large" deformations (within the limits of linear elasticity theory), it is appropriate to extend the asymptotic solution up to next higher order.

In Figs. 6 and 7 we investigate limits of validity of the expansion. Here the solutions, up to order δ, of the asymptotic model are drawn together with the results of the full system of Eqs. (9)–(12), for two cases, $\delta = 0.1$ and 0.3, corresponding, respectively, to $p_{infusion} = 43.75$ mmHg and $p_{infusion} = 108.75$ mmHg. Case 1 has been considered in both figures. The agreement is good, despite the fact that the larger value of $p_{infusion}$ greatly exceeds those commonly encountered in applications; such a large value of δ is of interest only to test the limitations of the asymptotic analysis. The validity of the latter statement stems also from [20] observation that the porosity ϕ of the interstitial matrix is approximately 0.2; this means that the pore velocity (equal to the Darcy flux q divided by ϕ) can be properly represented by the expansion proposed only when δ is much smaller than 0.2. In the results shown here we have fixed K_0 to the value of 3×10^{-6} cm^2/(mmHg s) which appears to provide flow rates of the agent at $r = a$ closer to the measured ones. The plots of the IFP resemble those presented by [6] for a similar configuration. The pressure decays over a small radial distance from the infusion site, and remains close to the effective vascular pressure over a range of r, before ultimately decaying to the value imposed at the tumor margin. When the infusion pressure is very large ($\delta = 0.3$) the agreement between the asymptotic solution at order δ and the full solution deteriorates but mildly, supporting the statement made at the beginning of Sec. 4. on the better-than-expected range of applicability of the asymptotic theory. As far as the hydraulic conductivity (computed with the asymptotic formulation) is concerned, it becomes negative very near the infusion boundary (cf. Fig. 7); one might imagine that second order in δ is needed to improve matters, but this is not consistent with linear elasticity theory which holds to first order in the deformation. In hindsight, the negative values of K are not of concern, they are irrelevant (just like the value of the pressure which appears to exceed the infusion pressure at $r = a$), since they occur (in the unphysical portion of the domain) where $r < a'$.

5 Closing Remarks

An asymptotic approach has been proposed for the study of the infusion of a therapeutic agent into a solid tumor, modeled as a poroelastic medium of conductivity anisotropically dependent on the material strain rate. In the model we have included fluid exchange with the capillary system, and observed the influence of variations of the vascular conductivity L_p on the results. In particular, when there is little or no fluid exchange between the inner tumor tissue and the vascular network, reduced radial displacements and flow rates are found as function of the radius, compared to the results of the original Starling's law model (for which L_p is

constant across the radius). For the conditions examined here it is notable that the flow rate Q systematically increases with r, an indication of the efficient delivery of the drug, related to the absent (or very reduced) reabsorption of fluid by the tumor capillaries.

By adopting values of the parameters which are commonly found in the literature, there is a reasonably good agreement of the computed infusion flow rates with the experimental results by McGuire et al. [12], for varying infusion pressures. The parameter that most strongly influences the results is the average hydraulic conductivity K_0 of the medium, whereas the radial distribution of K plays a relatively minor role. Given the large scatter of data present in the literature for K_0, there seems to be little need in coupling the elastic deformation of the fluid with the hydraulic properties of the interstitium: the leading order, uncoupled, solution is sufficiently accurate, at least for sufficiently low values of the infusion pressure. The situation is obviously different should very large strains of the tissue occur.

Several lines of research arise in light of the results reported here. One is based on the use of nonlinear theory for the behavior of materials undergoing strong displacements. The neo-Hookean material, often used for modeling elastin and collagen, could possibly be used, as well as the Fung-elastic constitutive model [21,22], appropriate for soft tissues characterized by pronounced mechanical anisotropy, highly nonlinear stress–strain relationships, large deformations, and viscoelasticity. Another avenue of research consists of developing a model which couples the intravascular and interstitial flow, reducing the need for model constants of uncertain determination. Progress along this line has been recently reported by Wu et al. [23,24]. Finally, even assuming that the tumor has a spheroidal shape, given the haphazard formation of cracks, hypoxic, and necrotic regions in tissues, it is estimated that only about 20% of the cases end up with a spherical distribution of flow and drugs [25], with irregular, three-dimensional infusion in all other cases. This is one of the major problems to overcome when modeling intratumoral infusion.

Acknowledgment

We gratefully acknowledge the insightful comments by Professor Fan Yuan, Dr. Rodolfo Repetto, and Dr. Marina Artuso.

References

[1] Baxter, L. T., and Jain, R. K., 1989, "Transport of Fluid and Macromolecules in Tumors. I. Role of Interstitial Pressure and Convection," Microvasc. Res., **37**, pp. 77–104.
[2] Boucher, Y. J., Kirkwood, M., Opacic, D., Desantis, M., and Jain, R. K., 1991, "Interstitial Hypertension in Superficial Metastatic Melanomas in Patients," Cancer Res., **51**, pp. 6691–6694.
[3] Roh, H. D., Boucher, Y., Kalnicki, S., Buchsbaum, R., Bloomer, W. D., and Jain, R. K., 1991, "Interstitial Hypertension in Carcinoma of Uterine Cervix in Patients: Possible Correlation With Tumor Oxygenation and Radiation Response," Cancer Res., **51**, pp. 6695–6698.
[4] Gutmann, R., Leunig, M., Feyh, J., Goetz, A. E., Messmer, K., Kastenbauer, E., and Jain, R. K., 1992, "Interstitial Hypertension in Head and Neck Tumors in Patients: Correlation With Tumor Size," Cancer Res., **52**, pp. 1993–1995.
[5] Shipley, R. J., and Chapman, S. J., 2010, "Multiscale Modelling of Fluid and Drug Transport in Vascular Tumours," Bull. Math. Biol., **72**, pp. 1464–1491.
[6] Smith, J. H., and Humphrey, J. A. C., 2007, "Interstitial Transport and Transvascular Fluid Exchange During Infusion Into Brain and Tumor Tissue," Microvascular Res., **73**, pp. 58–73.
[7] Zhang, X.-Y., Luck, J., Dewhirst, W. M., and Yuan, F., 2000, "Interstitial Hydraulic Conductivity in a Fibrosarcoma," Am. J. Physiol., **279**, pp. H2726–H2734.
[8] Netti, P. A., Baxter, L. T., Boucher, Y., Skalak, R. K., and Jain, R. K., 1995, "A Poroelastic Model for Interstitial Pressure in Tumors," Biorheology, **32**, p. 346.
[9] Sarntinoranont, M., Rooney, F., and Ferrari, M., 2003, "Interstitial Stress and Fluid Pressure Within a Growing Tumor," Ann. Biomed. Eng., **31**, pp. 327–335.
[10] Lai, W. M., and Mow, V. C., 1980, "Drag-Induced Compression of Articular Cartilage During a Permeation Experiment," Biorheology, **17**, pp. 111–123.
[11] Barry, S. I., and Aldis, G. K., 1990, "Comparison of Models for Flow Induced Deformation of Soft Biological Tissues," J. Biomech., **23**, pp. 647–654.
[12] McGuire, S., Zaharoff, D., and Yuan, F., 2006, "Nonlinear Dependence of Hydraulic Conductivity on Tissue Deformation During Intratumoral Infusion," Ann. Biomed. Eng., **34**, pp. 1173–1181.
[13] Basser, P. J.,. 1992, "Interstitial Pressure, Volume, and Flow During Infusion Into Brain Tissue," Microvasc. Res., **44**, pp. 143–165.
[14] Pries, A. R., Cornelissen, A. J. M., Sloot, A. A., Hinkeldey, M., Dreher, M. R., Höpfner, M., Dewhirst, M. W., and Secomb, T. W., 2009, "Structural Adaptation and Heterogeneity of Normal and Tumor Microvascular Networks," PLoS Comput. Biol., **5**(5), pp. e1000394.
[15] Truskey, G. A., Yuan, F., and Katz, D. F., 2009, *Transport Phenomena in Biological Systems*, 2nd ed., Pearson Prentice Hall Bioengineering, Upper Saddle River, NJ.
[16] Baxter, L. T., and Jain, R. K., 1990, "Transport of Fluid and Macromolecules in Tumors. II. Role of Heterogeneous Perfusion and Lymphatics," Microvasc. Res., **40**, pp. 246–263.
[17] Bonfiglio, A., Leungchavaphongse, K., Repetto, R., and Siggers, J. H., 2010, "Mathematical Modeling of the Circulation in the Liver Lobule," ASME J. Biomech. Eng., **132**, p. 111011.
[18] Swabb, E. A., Wei, J., and Gullino, P. M., 1974, "Diffusion and Convection in Normal and Neoplastic Tissues," Cancer Res., **34**, pp. 2814–2822.
[19] McGuire, S., and Yuan, F., 2001, "Quantitative Analysis of Intratumoral Infusion of Color Molecules," Am. J. Physiol., **281**, pp. H715–H721.
[20] Jain, R. K., 1987, "Transport of Molecules in the Tumor Interstitium: A Review," Cancer Res., **47**, pp. 3039–3051.
[21] Fung, Y. C., 1993, *Biomechanics. Mechanical Properties of Living Tissues*. Springer, Berlin.
[22] Sun, W., and Sacks, M. S., 2005, "Finite Element Implementation of a Generalized Fung-Elastic Constitutive Model for Planar Soft Tissues," Biomech. Model Mechanobiol., **4**, pp. 190–199.
[23] Wu, J., Long, Q., Xu, S., and Padhani, A. R., 2009, "Study of Tumor Blood Perfusion and its Variation Due to Vascular Normalization by Anti-Angiogenic Therapy Based on 3D Angiogenic Microvasculature," J. Biomech., **42**, pp. 712–721.
[24] Wu, J., Xu, S., Long, Q., Collins, M. W., König, C. S., Zhao, G., Jiang, Y., and Padhani, A. R., 2008, "Coupled Modeling of Blood Perfusion in Intravascular, Interstitial Spaces in Tumor Microvasculature, J. Biomech., **41**, pp. 996–1004.
[25] Yuan, F., 2011, personal communication.